

Sub-natural resonances due to ground state coherence in ^6Li

J Fuchs^{1,2}, G J Duffy^{1,2}, W J Rowlands^{1,2} and A M Akulshin²

¹ ARC Centre of Excellence for Quantum Atom Optics

² Centre for Atom Optics and Ultrafast Spectroscopy, Swinburne University of Technology, Melbourne, Victoria 3122, Australia

E-mail: jfuchs@swin.edu.au

Abstract. We report sub-Doppler and sub-natural linewidth spectroscopy of ^6Li on the D1 and D2 lines in both a vapour cell and an atomic beam. Electromagnetically induced transparency is created using co-propagating mutually coherent laser beams with a frequency difference equal to the hyperfine ground state splitting of 228.2 MHz. The effects of various optical polarization configurations and applied magnetic fields are investigated. In addition, we present an optical Ramsey spectroscopy technique which further reduces the observed resonance width.

PACS numbers: 32.10.Fn, 32.30.Jc, 32.80.Qk

Submitted to: *J. Phys. B: At. Mol. Phys.*

1. Introduction

Laser spectroscopy of the lithium D lines has attracted much attention in recent years (see e.g., (Olivares *et al* 1998, Walls *et al* 2003, Magnus *et al* 2005) and references therein). Accurate measurements of isotope shifts together with theoretical calculations of both isotopes of the simplest alkali element could improve the precision of important fundamental constants such as the fine structure constant (Wijngaarden 2005). Comparison of theoretical calculations of atomic hyperfine splitting with experimental results may provide a test for QED (Ashby *et al* 2003).

Lithium has two stable isotopes, ${}^6\text{Li}$ (natural abundance 7.5 %) and ${}^7\text{Li}$ (natural abundance 92.5 %). ${}^6\text{Li}$ is the only stable fermionic alkali isotope apart from the naturally rare ${}^{40}\text{K}$. The quantum statistics of fermions dramatically differs from the statistics of bosons and in several experiments worldwide this interesting behaviour has been explored (see e.g., (Jochim *et al* 2003, Zwierlein *et al* 2003, Bourdel *et al* 2004)). In previous studies (Walls *et al* 2003, Olivares *et al* 1998) spectroscopy of the $2^2P_{1/2,3/2}$ levels of ${}^6\text{Li}$ have been carried out using a linear Doppler-free method, based on a collimated atomic-beam and a heat pipe. In both cases the spectral resolution is limited by the natural linewidth of the optical transition. More recently Magnus *et al* (Magnus *et al* 2005) reported the first study of Electromagnetically Induced Transparency (EIT) on the D1 and D2 lines of ${}^7\text{Li}$ in a vapour. In this paper we present sub-Doppler and sub-natural linewidth spectroscopy of ${}^6\text{Li}$ performed on both the D1 and D2 lines using several nonlinear techniques.

Light-induced ground state coherence effects such as EIT (Harris 1997) can provide spectral resolution well below the natural width of the atomic transition. Coherence effects in alkali atoms with half-integer total angular momentum ($F=J+I$, $J=L\pm 1/2$) have not, to our knowledge, been previously investigated. The integer nuclear spin ($I=1$) of ${}^6\text{Li}$ makes it an interesting atomic species for coherence spectroscopy. Additionally we use a Ramsey-type configuration of coherence spectroscopy in an atomic beam to reduce time of flight broadening.

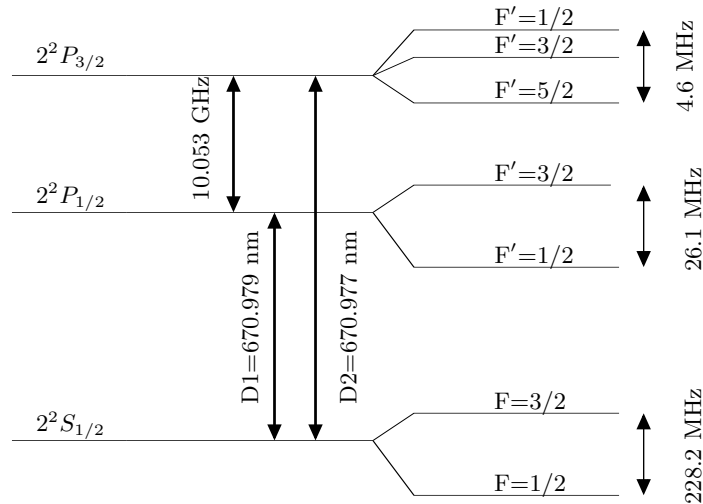


Figure 1. A schematic energy level diagram for ${}^6\text{Li}$.

A schematic diagram of the relevant atomic energy levels is shown in figure 1. The strongest optical transitions of ${}^6\text{Li}$ are two electric dipole transitions $2^2S_{1/2} \rightarrow 2^2P_{1/2}$ (D1 line) and $2^2S_{1/2} \rightarrow 2^2P_{3/2}$ (D2 line) which are separated by a fine splitting of ~ 10 GHz. The hyperfine splitting of the $2^2S_{1/2}$ ground state is 228.2 MHz and the hyperfine splitting of the excited $2^2P_{1/2}$ state is 26.1 MHz (Walls *et al* 2003). The hyperfine splitting of the $2^2P_{3/2}$ state is smaller than the 6 MHz natural width of the optical transition.

2. Saturation Spectroscopy

Saturation spectroscopy in a lithium vapour cell (figure 2) provides sub-Doppler reference resonances for laser frequency stabilization. An external cavity diode laser (ECDL) (Toptica DL 100) is used as the source of the resonant optical field which has an output power of 15 mW and a linewidth of approximately 1 MHz. Using the so-called feed-forward technique, where both the diode current and the grating position are varied, a fine frequency tuning range of over 20 GHz can be obtained. The vapour cell consists of a stainless steel crossed tube configuration with a flexible bellow construction and viewports on each end of the 30 cm horizontal arm. Using a thermocoax element the centre part of the vapour cell is heated to 350 °C yielding a maximum unsaturated absorption of about 20%. At this temperature the Doppler width is 3.5 GHz. Lithium vapour is limited by its mean free path to the centre part of the tube, protecting the viewports from becoming coated with lithium. To further reduce this problem we heat the viewports to 120° C.

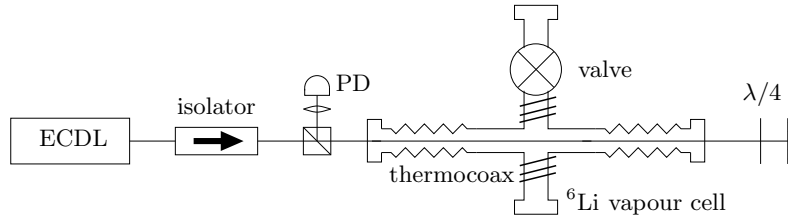


Figure 2. Experimental set-up for saturation spectroscopy in a vapour cell.

In our saturation spectroscopy set-up (figure 2) the counter-propagating retroreflected laser beam, the probe, is focused onto a photodiode. Typically, the incident laser power is 1.5 mW and has a beam diameter of 2 mm. Figure 3 shows typical Doppler-free spectra of ${}^6\text{Li}$. A frequency scan over both the D1 and D2 lines is shown in figure 3 (a) whereas (b) and (c) represent a close-up of the D1 and D2 lines respectively. The outer two peaks in (b) correspond to the D1 $F = 3/2 \rightarrow F' = 1/2, 3/2$ and $F = 1/2 \rightarrow F' = 1/2, 3/2$ transitions whereas the outer peaks in (c) correspond to the D2 $F = 3/2 \rightarrow F' = 5/2, 3/2, 1/2$ and $F = 1/2 \rightarrow F' = 3/2, 1/2$ transitions respectively. The reduction in absorption of the probe at these outer peaks is due to the saturation of the transition by the pump beam. The enhancement in absorption of the crossover peak is due to compensation of optical hyperfine pumping, which occurs when the pump and probe laser are resonant with both ground state sublevels at the same time. This crossover resonance is strong if the hyperfine splitting of the ground state is smaller than the Doppler width (Velichansky *et al* 1980) and does not exist for other alkali atoms, such as rubidium or cesium, where the Doppler width is typically

much smaller than the ground state hyperfine splitting. In figure 3 (b) the incident optical power was reduced to $150\text{ }\mu\text{W}$ to increase the resolution. Although it was not possible to resolve the hyperfine splitting of the $2^2P_{1/2}$ state, we could partly resolve the crossover between the transitions from the $F = 1/2$ and $F = 3/2$ ground states (figure 3 (b)).

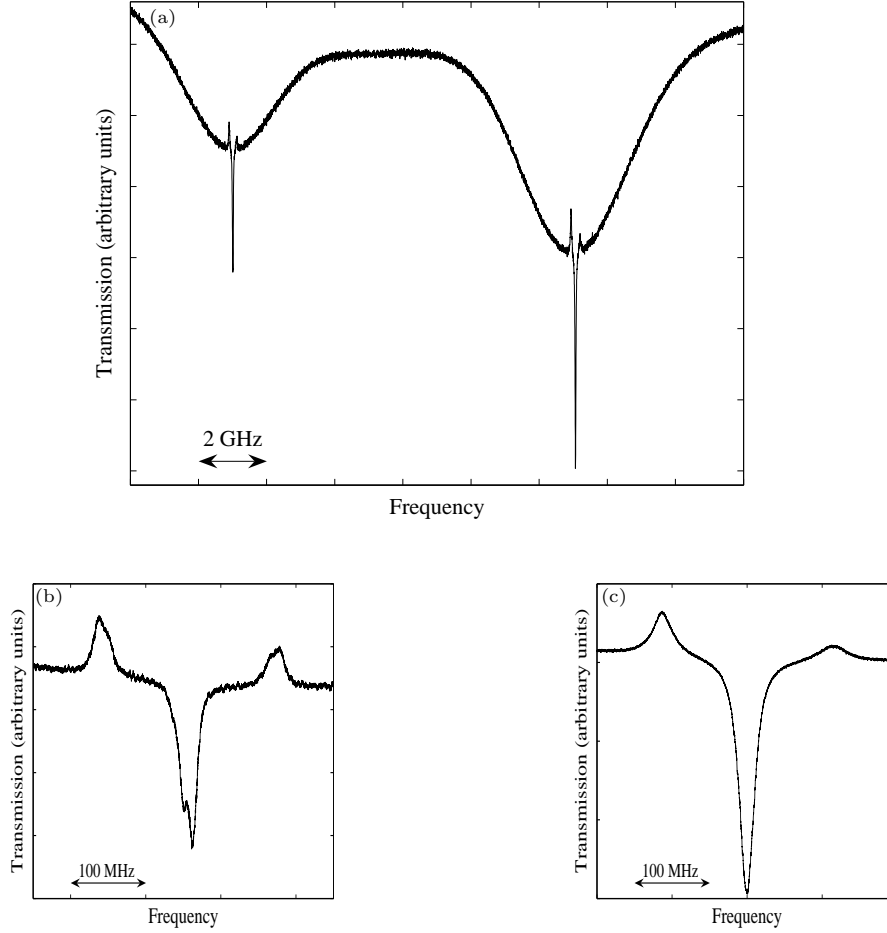


Figure 3. Doppler-free spectrum of ${}^6\text{Li}$. (a) Frequency scan over both the D1 and D2 lines. (b) and (c) A close-up of the scan across the D1 and D2 line respectively. The outer two peaks in (b) correspond to the $F = 3/2 \rightarrow F' = 1/2, 3/2$ and $F = 1/2 \rightarrow F' = 1/2, 3/2$ transitions respectively, whereas the outer peaks in (c) correspond to $F = 3/2 \rightarrow F' = 5/2, 3/2, 1/2$ and $F = 1/2 \rightarrow F' = 3/2, 1/2$ transitions. The hyperfine structure of the $2^2P_{3/2}$ state is unresolved.

Saturation spectroscopy of lithium vapour provides an excellent frequency reference for our experiments in an atomic beam. To frequency stabilize the laser we modulate the laser frequency by dithering the laser current. Using a lock-in amplifier the derivative of the absorption profile is obtained. In most experiments

the ECDL is locked to the crossover dip. To achieve a stable lock, we require a large crossover amplitude. This is obtained by applying relatively high laser intensities in our saturation spectroscopy which ultimately broadens the width of the crossover dip. When applying these higher intensities the structure in figure 3 (b) is no longer observed and resembles the spectroscopy of the D2 line (figure 3 (c)). The width of the crossover peak in figure 3 (c) is ≈ 25 MHz. The contrast ratio of the crossover peak with respect to the Doppler broadened resonance is $\approx 100\%$.

3. Vapour Cell EIT

EIT is a phenomenon in which an opaque atomic medium is turned into a transparent one in the presence of a control laser field (Harris 1997). When two Zeeman sub-levels or two hyperfine levels in an atomic ground state are coupled by light to a common excited state, the interference between amplitudes of alternative transition paths can substantially reduce the absorption due to destructive interference. The atoms are pumped by the laser light into a coherent superposition of the ground state sublevels which constitutes a non-absorbing state decoupled from the laser field. The absorption of the probe exhibits a narrow dip that has a sub-natural linewidth ultimately determined by the relaxation time of the ground state sublevels. The refractive index of the coherent atomic medium reveals extremely steep normal dispersion in the vicinity of the EIT resonance, so that the group velocity of light in such an atomic medium can be dramatically reduced (Schmidt *et al* 1996). EIT is of great interest due to its wide application in lasing without inversion (Zibrov *et al* 1995), control of light propagation (slow light) (Matsko *et al* 2001) and enhanced Kerr nonlinearity (Harris and Hau 1999). The concept of a non-absorbing dark state is the key basis of light storage (Lukin 2003).

The ultimate width of an EIT resonance also depends on the mutual coherence of the probe and control laser fields (Arimondo 1996). Ultrahigh spectral resolution of EIT resonances in Cs and Rb vapour with large ground state splitting requires expensive high frequency AOMs or two phase-locked lasers to couple both hyperfine levels to a common excited state. Phase locking with precise frequency offset is experimentally not simple. However, in the case of lithium mutually coherent probe and control fields can be easily prepared from the same laser using low-cost AOMs because the ground state splitting is relatively small.

With only a single laser frequency present, the width of the absorption features due to velocity selective optical pumping or direct saturation of optical transitions are limited by the natural linewidth of ≈ 6 MHz. By tailoring the optical frequencies present we performed sub-natural spectroscopy in both a vapour cell and an atomic beam. To obtain hyperfine ground state coherence we use mutually coherent laser fields whose frequencies are separated by the hyperfine splitting of the ground state. Although EIT can easily be obtained using only one laser and standard acousto-optical modulators (AOMs) to shift the frequencies, we injection lock three additional slave lasers as seen in figure 4 to provide more laser power which will be required for our future experiments.

Figure 4 shows the experimental set-up used for EIT experiments in the vapour cell. The ECDL (master laser) is used to injection lock three diode lasers (slaves). The injecting light is coupled via optical isolators. The master laser is tuned to either the D1 or D2 line and is not actively stabilized since its long-term drift is small compared to the Doppler width. Radiation of one of the slaves is used as a pump beam for

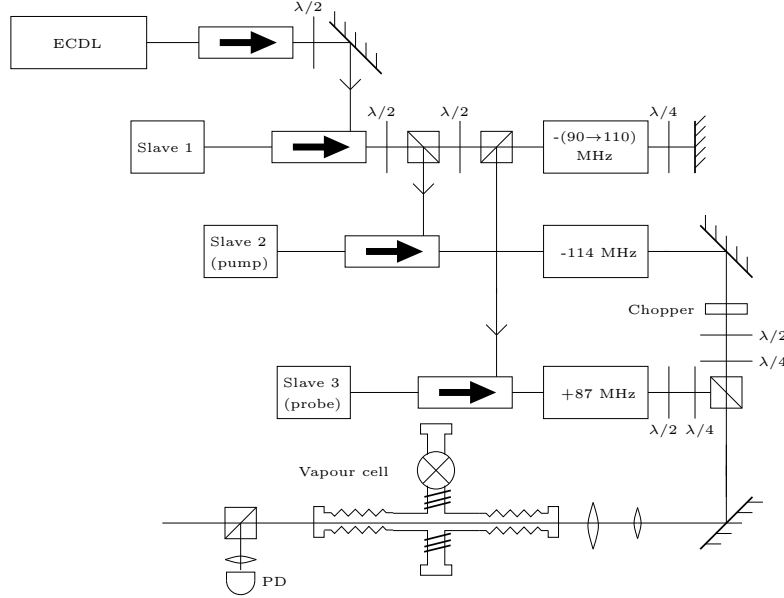


Figure 4. Experimental set-up for the EIT experiments in the vapour cell. The ECDL is free running and tuned to the Doppler profile of either the D1 or the D2 line. Three slave lasers were injection locked to the master laser. Where necessary, the frequencies were shifted using AOMs. The frequency difference sweep of pump and probe laser was generated by the AOM in double pass. The typical frequencies used in the AOMs are shown in the above figure.

coupling states between the ground state $F = 1/2$ and the excited levels in the D1 or D2 line. Laser light from another slave which is resonant to the $F = 3/2 \rightarrow F'$ transitions (either D1 or D2 line) is used as a weak probe, whose transmission through the ^6Li vapour was recorded. The optical frequencies are shifted accordingly using AOMs. One of the AOMs is in a double-pass configuration where the frequency can be swept without changing the beam alignment. The polarizations of the pump and probe beams can be independently set using polarizers and $\lambda/2$ or $\lambda/4$ waveplates. For the results shown here, both beams are linearly polarized and orthogonal to each other. They are overlapped on a non-polarizing beam splitting cube and expanded to a beam diameter of 5 mm. The pump and probe are sent through the vapour cell with intensities of 8 mW/cm^2 and 2 mW/cm^2 respectively. The probe light is picked off using a polarizing beam splitter and detected using a photodiode. The probe laser frequency is scanned over $\approx 25 \text{ MHz}$ while the frequency of the pump laser is fixed. To improve the signal to noise ratio the pump is amplitude modulated by means of an mechanical chopper (1 kHz) and the probe is detected using a lock-in amplifier.

3.1. Results

Figure 5 shows absorption plots of the D1 and D2 lines as a function of frequency difference where the pump and probe beams are collinear. With no externally applied magnetic field a single absorption dip is observed (figure 5 (a) and 5 (d)). Applying

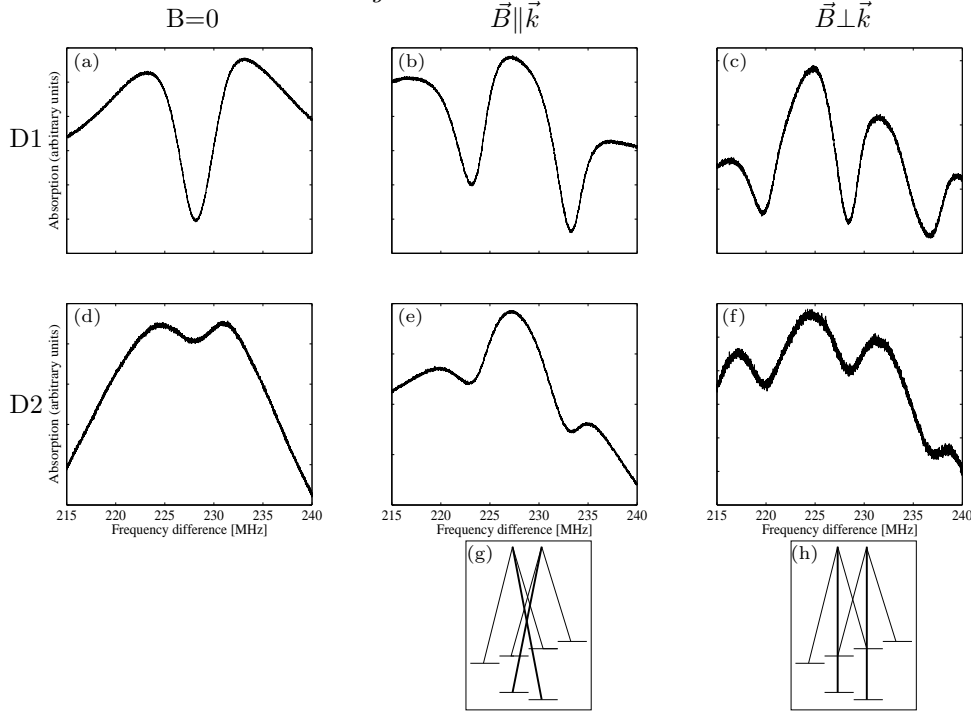


Figure 5. Absorption of the D1 (a-c) and D2 (d-f) line as a function of frequency difference between the pump and probe. (a) and (d): $B = 0$, (b) and (e): have a magnetic field parallel to the laser light. (c) and (f) have a magnetic field perpendicular to the laser light. (g)((h)) shows the transitions responsible between the ground state Zeeman sublevels for each of the resonances in (b+e) ((c+f)). Note, the thicker lines represent the pump transitions. A magnetic field of ≈ 5 G was applied to both the perpendicular and parallel fields.

a magnetic field, either parallel or perpendicular to the laser light, removes the degeneracy of Zeeman levels resulting in the addition of further dips. The spectra in figure 5 show six different plots corresponding to the D1 or D2 line with either parallel or perpendicular magnetic fields applied to them. For plots (a-c) ((d-f)), the master laser is tuned to the D1 (D2) transition line. When a magnetic field of a few Gauss (≈ 5 G) is applied parallel to the laser light ($\vec{B} \parallel \vec{k}$, where \vec{k} is the wavevector) as in figure 5 (b) and 5 (e), the width of the resonance is ≈ 3 MHz which is sub-natural. This width is limited by magnetic field inhomogeneities, finite interaction (transit) time and collisions with residual gases. Both absorption dips are shifted by $\Delta = \mu_B g_F B / h$ to either side of the zero B-field resonance, where μ_B is the Bohr magneton, h is Planck's constant and g_F is the Landé factor. In figure 5 (c) and 5 (f) the applied magnetic field is perpendicular to the laser light ($\vec{B} \perp \vec{k}$) and parallel to the pump laser polarization. Both outer dips are shifted 2Δ from the unshifted centre dip. In figure 5 (c) the widths of the outer dips are 25% larger than the width of the centre dip. This is due to spatial inhomogeneities in the magnetic field. We reduced the intensities of the pump and probe lasers but observed no change in the width of the EIT peaks which implies that they are not limited by power broadening. The experiments were repeated for σ^+ and σ^- polarization of pump and probe. The

structure and resonance widths were unchanged, although the peaks were somewhat less pronounced.

4. Atomic Beam EIT

The spectroscopy of atoms in a metal vapour cell has the limitations of randomly directed velocities (i.e. Doppler broadening), field inhomogeneities and high collision rates. To improve the resolution of EIT resonances measurements were made using a collimated atomic beam. A schematic diagram of the set-up used with an atomic beam is shown in figure 6. Ultra high vacuum is achieved in a glass cell which has outer dimensions of $3\times 3\times 12\text{ cm}^3$ with a wall thickness of 3 mm. The anti-reflection coated cell (for 670 nm) was wrapped in μ -metal to reduce stray magnetic fields. Isotopically enriched ^6Li atoms are evaporated from an oven at a temperature of 450°C to produce a thermal atomic beam. At this temperature the pressure was 2×10^{-10} Torr in the glass cell with an expected ^6Li vapour pressure of 4×10^{-4} Torr in the oven. The divergence of the atomic beam is 5.5 mrad and the diameter of the beam at the centre of the probe region is 7 mm. Since the transverse Doppler width was reduced considerably it was necessary to frequency stabilize the master laser by actively locking to the crossover of the saturated absorption line. The pump and probe frequencies for the EIT experiments were obtained using the same system of AOMs used for EIT in the vapour cell. The pump and probe beams were overlapped on a non-polarizing beam splitting cube and then expanded to a beam diameter of 18 mm. Fluorescence from atoms in the probe region was detected using a photomultiplier tube. The pump and probe intensities were 1.4 mW/cm^2 for both beams.

4.1. Results

The collimated atomic beam showed a much narrower transverse Doppler width of 20 MHz compared to $\approx 3.5\text{ GHz}$ obtained in the vapour cell. Therefore, the hyperfine splitting of the $2^2\text{P}_{1/2}$ state of 26.1 MHz can be resolved. Figure 7 shows a plot of fluorescence of the D1 line as a function of frequency difference. In this figure the probe laser is scanned over both the $F = 3/2 \rightarrow F' = 1/2$ and $F = 3/2 \rightarrow F' = 3/2$ transitions whereas the pump laser has a fixed frequency tuned to the $F = 1/2 \rightarrow F' = 1/2$ (a) or $F = 1/2 \rightarrow F' = 3/2$ (b) transition. The EIT dip is more pronounced when the fixed laser is tuned to the $F' = 3/2$ state which is due to the larger transition amplitude. For this reason we performed all of the subsequent experiments with the pump laser tuned to the $F = 1/2 \rightarrow F' = 3/2$ transition.

Figure 8 shows several EIT resonances obtained for various polarizations with and without an applied B-field ($\approx 2\text{ G}$) along the atomic beam. In 8 (a) and 8 (b) the polarization of both lasers is linear and perpendicular to each other. The two outer peaks in (b) are both shifted by 2Δ from the zero field resonance which is consistent with the allowed transitions depicted in (c). Orthogonal circular polarizations were used for the pump and probe to obtain the plots in figure 8 (d) and 8 (e). With the B-field perpendicular to the laser, all transitions are allowed (figure 8 (f)) and it should be possible to observe five dips (for which we only observe three), each separated by Δ . In (g) and (h) the polarization of both laser beams are aligned parallel to each other and orthogonal to the magnetic field. Only two Λ -systems are allowed in this configuration (figure 8 (i)). The two resulting EIT resonances are both shifted by Δ

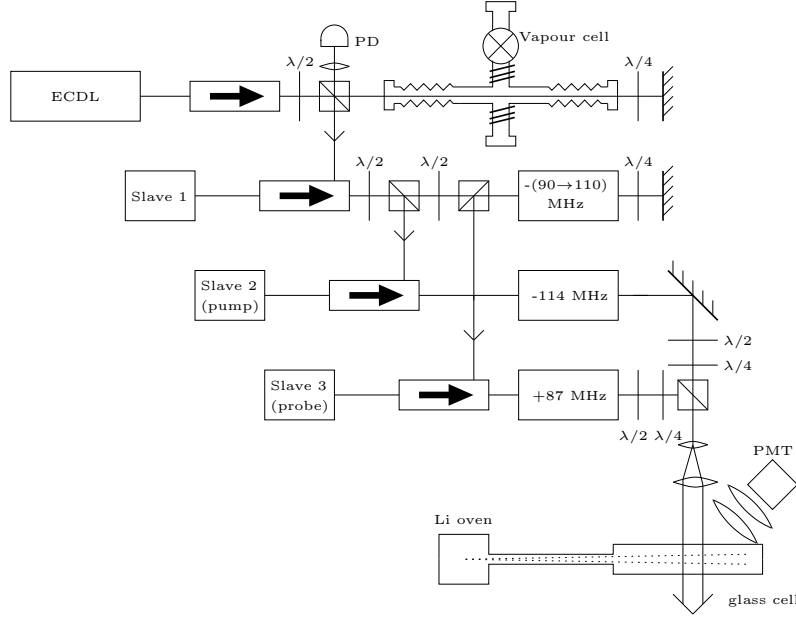


Figure 6. Experimental set-up for the EIT experiments using an atomic beam. The ECDL is frequency locked to the crossover of the saturated absorption signal. Three slave lasers were injection locked to the master laser. The subsequent laser set-up is the same as the set-up used for the experiments in the vapour cell. Typical frequencies used in the AOMs are shown in the above figure.

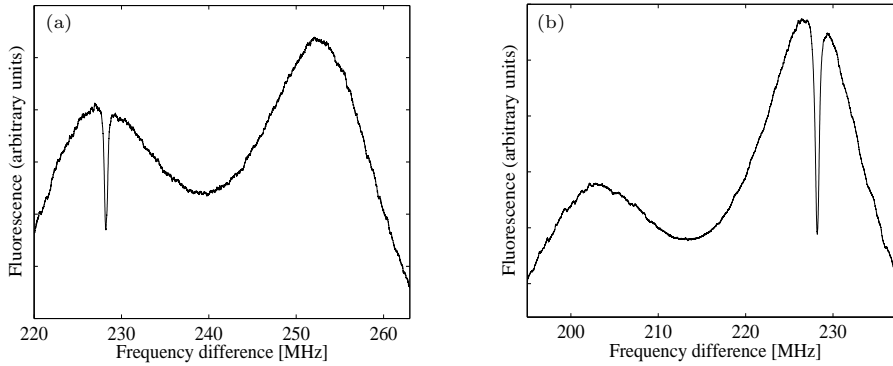


Figure 7. Fluorescence of the D1 line. Probe laser is scanned over both the $F = 3/2 \rightarrow F' = 1/2$ and $F = 3/2 \rightarrow F' = 3/2$ transitions. (a) Fixed pump laser tuned to $F = 1/2 \rightarrow F' = 1/2$ transition (b) Fixed pump laser tuned to $F = 1/2 \rightarrow F' = 3/2$ transition.

to either side of the zero-magnetic field resonance. Similar results were obtained for the D2 line.

The EIT resonances in the ^6Li beam (figures 7 and 8) have a width of ≈ 300 kHz.

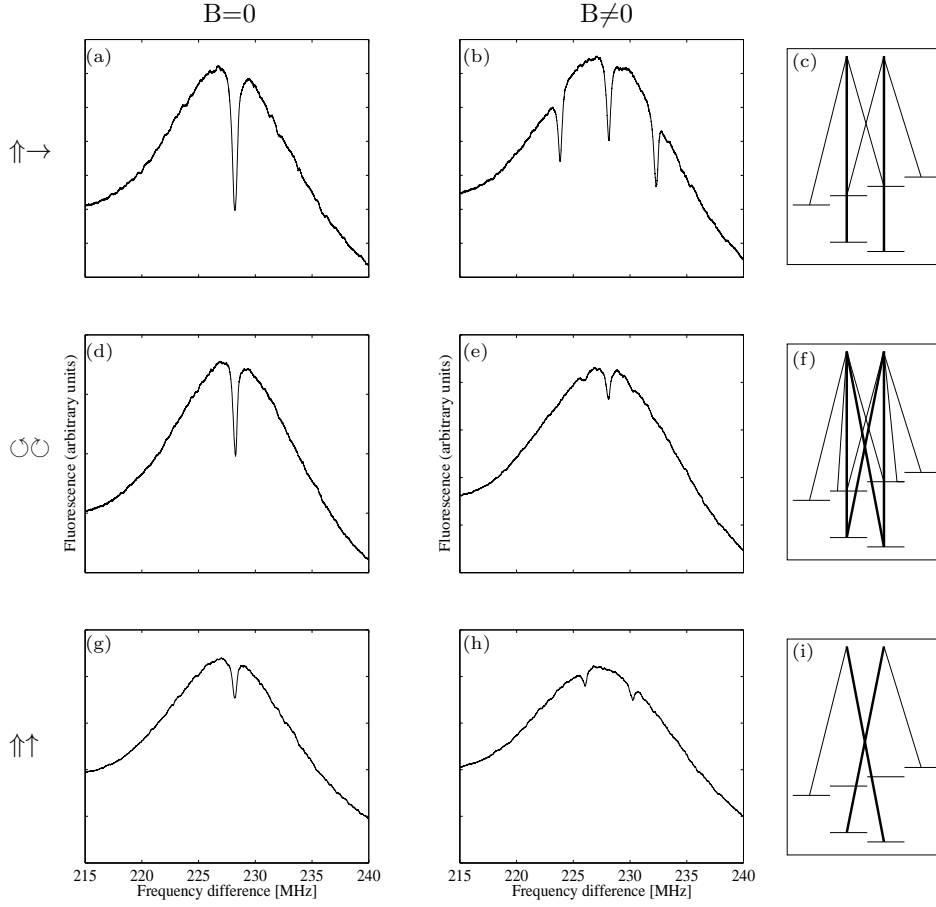


Figure 8. Fluorescence of the D1 line as a function of frequency difference. Fixed pump laser tuned to $F = 1/2 \rightarrow F' = 3/2$. (a), (d) and (g): $B=0$, (b), (e) and (h): $B \approx 2$ G. (a) and (b): linear perpendicular polarization, (d) and (e): σ^+ , σ^- polarization, (g) and (h): linear parallel polarization. The transitions shown in (c), (f) and (i) are responsible for each of the corresponding resonances to their left. Note, the thicker lines represent the pump transitions.

This is a factor of 10 reduction compared to the vapour cell experiments. To get a better understanding of the broadening of our EIT resonances in the atomic beam we investigated the dependence of the width on the laser intensity of the pump laser, as shown in figure 9 (a). In addition, the amplitudes of the EIT resonances are shown. Note, that the intensity of the probe laser is kept fixed at 1 mW/cm^2 . We observe a linear dependence of both the amplitude and the resonance width on the laser intensity. The linear behaviour of the resonance width is expected when power broadening becomes significant (Agap'ev 1993). Extrapolation gives a low-intensity limit of 190 kHz.

Additional broadening comes from the limited interaction time of the atoms with the light field (transit-time broadening). This was studied by measuring the resonance width for different laser beam cross-sections and the results are shown in figure 9(b). In

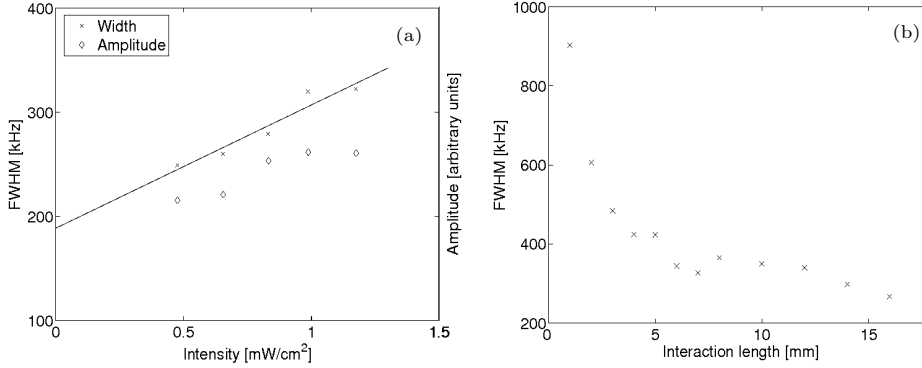


Figure 9. (a) Width of observed EIT resonance versus pump laser intensity. The intensity of the probe laser was fixed at 1 mW/cm^2 . The amplitude of the resonances as a function of laser intensity is also shown. (b) Width of observed EIT resonance versus interaction length. The sum of the laser intensities was 1.7 mW/cm^2 . In (a) and (b) EIT was achieved using the $^2\text{P}_{1/2}$, $F' = 3/2$ excited state and the polarization of the laser light was linear and perpendicular to each other.

our work the sum of the laser intensities was kept fixed at 1.7 mW/cm^2 . A significant increase could be observed for interaction lengths smaller than 5 mm. However, for a beam diameter of 18 mm used in all other experiments the broadening due to the transit time is negligible relative to the contribution of power broadening and magnetic field inhomogeneities.

5. Ramsey Spectroscopy

Further reduction of EIT resonance widths was achieved using Ramsey spectroscopy (Ramsey 1989). In this technique atoms or molecules in a beam pass two spatially separated interaction regions. Optical Ramsey fringes were observed on beams of Na and Cs atoms pumped into coherent non-absorbing states (Thomas *et al* 1982, Hemmer *et al* 1993).

Here, a coherent superposition of the $F = 1/2$ and $F = 3/2$ ground states is prepared in a light field. The laser field consists of two co-propagating laser beams which are resonant with the $F = 1/2 \rightarrow F' = 3/2$ and $F = 3/2 \rightarrow F' = 3/2$ transitions. After some time of flight the state is probed in a second interaction region consisting of the same two frequencies. Similar to the EIT experiments described previously, the laser resonant with the $F = 1/2 \rightarrow F' = 3/2$ transition is kept fixed while the other frequency is swept over the $F = 3/2 \rightarrow F' = 3/2$ transition.

In our experiment the two interaction regions were separated by $L = 7.7\text{ mm}$. This was achieved by using only one laser beam in which the complete central vertical portion was blocked. Figure 10 shows a plot of fluorescence as a function of frequency difference. The intensities for both pump and probe were 2 mW/cm^2 . The polarization of both beams were linear and perpendicular to each other. To amplify the Ramsey fringes the laser light in the first interaction region was chopped, while the fluorescence of the probe region was detected on a photo multiplier tube using a lock-in amplifier.

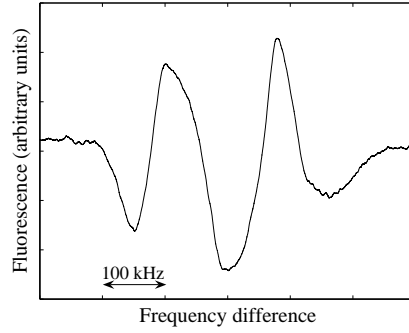


Figure 10. Optical Ramsey fringes of two co-propagating laser beams in a Raman-type configuration.

The obtained width (FWHM) of the resonance was narrower than 100 kHz which is consistent with calculations based on a mean atomic velocity $v \approx 1600 \text{ ms}^{-1}$ and laser field separation L ; $\Delta\nu = v/(3L) = 70 \text{ kHz}$ (Demtröder 2003).

6. Summary

We have reported high-resolution spectroscopy of ^6Li using several techniques, including saturated absorption, electromagnetically induced transparency in both the vapour cell and atomic beam, and optical Ramsey spectroscopy. The saturated absorption in an atomic vapour is limited in resolution by both the natural linewidth of 6 MHz and the unresolved hyperfine splitting, but can be used as a frequency reference for stabilizing diode laser systems. A frequency stabilized laser system with precise frequency tuning in the range of the ground state hyperfine splittings was used. Resonant light with two frequency components was used to form coherences between the two hyperfine levels in the ^6Li ground state for the first time, allowing absorption features as narrow as 200 kHz to be observed. The effects of various optical polarization configurations and applied magnetic fields were investigated, and these were readily interpreted using conventional EIT theory. Additional EIT experiments using a Ramsey type separated-field geometry showed further reduction in the resonance widths.

As an alkali atom with integer nuclear spin, ^6Li presents an interesting system to investigate coherence effects such as EIT. Our initial investigations are consistent with results obtained using other alkali atoms, such as rubidium and cesium. Interesting effects involving coherence spectroscopy may be expected for other coherence phenomena such as coherences between Zeeman states within a hyperfine level.

Acknowledgments

We would like to thank Peter Hannaford for his useful advice and discussions. This project is supported by the Australian Research Council Centre of Excellence for Quantum-Atom Optics and Swinburne University of Technology.

References

- Agap'ev B D, Gornyi M B, Matisov B G, Rozhdestvenskii Yu V 1993 *Usp. Fiz. Nauk* **163** 1–36
- Arimondo E 1996 *Prog. Opt.* **30** 257–354
- Ashby R, Clarke J J, van Wijngaarden W A 2003 *Eur. J. Phys.* **23** (3) 327–331
- Bourdel T, Khaykovich L, Cubizolles J, Zhang J, Chevy F, Teichmann M, Tarruell L, Kokkelmans S and Salomon C 2004 *Phys. Rev. Lett.* **93** 050401–050404
- Demtröder W 2003 *Laser spectroscopy: Basic concepts and Instrumentation* vol 3 (New Delhi: Springer-Verlag)
- Harris S E 1997 *Physics Today* **50**(7) 32
- Harris S E and Hau L 1999 *Phys. Rev. Lett.* **82** 4611–4614
- Hemmer P R, Shahriar M S, Lamela-Rivera H, Smith S P, Bernacki B E and Ezekiel S 1993 *J. Opt. Soc. Am. B* **10** 1326
- Jochim S, Bartenstein M, Altmeyer A, Hendl G, Reidl S, Chin C, Hecker-Denschlag J and Grimm R 2003 *Science* **302** 2101
- Lukin M D 2003 *Rev. Mod. Phys.* **75** 457–472
- Magnus F, Boatwright A L, Flodin A and Shiell R C 2005 *J. Opt. B:Quantum Semiclass. Opt.* **7** 109–118
- Matsko A B, Kocharovskaya O, Rostovtsev Y, Welch G R, Zibrov A S and Scully M O 2001 *Advances in Atomic Mol. and Opt. Phys.* **46** 191–242
- Olivares I E, Duarte A E, Lokajczyk T, Dinklage A and Duarte F J 1998 *J. Opt. Soc. Am. B.* **15** 1932–1939
- Ramsey N F 1989 *Molecular Beams* 2nd Edn, Clarendon, Oxford
- Schmidt O, Wynands R, Hussein Z and Meschede D 1996 *Phys. Rev. A* **53** R27–R30
- Thomas J E, Hemmer P R, Ezekiel S, Leiby C C Jr., Picard R H and Willis C R 1982 *Phys. Rev. Lett.* **48** 867–870
- Velichansky V L, Zibrov A S, Kargopol'tsev V S, Kachurin O R, Nikitin V V, Sautenkov V A, Kharisov G G and Tyurikov D A 1980 *Sov. Journal of Quantum Electronics* **10** 1244
- Walls J, Ashby R, Clarke J J, Lu B and van Wijngaarden W A 2003 *European Physics Journal D* **22** 159–162
- van Wijngaarden W A 2005 *Can. J. Phys.* **83** 327
- Zibrov A S, Lukin M D, Nibonov D E, Hollberg L, Scully M O, Velichansky V L and Robinson H G 1995 *Phys. Rev. Lett.* **75** 1499–1502
- Zibrov A S, Lukin M D and Scully M O 1999 *Phys. Rev. Lett.* **83** 4049–4052
- Zwierlein M W, Stan C A, Schunck C H, Raupach S M F, Gupta S, Hadzibabic Z and Ketterle W 2003 *Phys. Rev. Lett.* **91** 250401–250404